EVS30 Symposium
Stuttgart, Germany, October 9 - 11, 2017

Degradation analysis and state of health estimation on lithium nickel manganese cobalt oxide (NMC) battery

Yi Li[1,2], Mohamed Abdel-Monem[1], Noshin Omar[1], Elise Nanini-Maury[2], Peter Van den Bossche[1], Joeri Van Mierlo[1]

[1] *Vrije Universiteit Brussel, MOBI Research Group, pleinlaan 2, 1050, Brussels, Belgium*

[2]*ENGIE LAB Laborelec, Rodestraat 125, B-1630 Linkebeek, Belgium*

Executive Summary

Battery ageing occurs throughout the entire life-time of the battery and limits its performance. Different operating conditions like working temperature, cycling depth, charge/discharge current rate, etc., lead to different degradation levels of the batteries. Having a profound understanding of battery ageing behaviour under various operating modes is helpful in improving battery life-time and hence making them economically more competitive. An accurate state of health (SoH) estimation of batteries is of great importance to the safety of entire systems, with this information we can adjust the operating modes to extend the battery lifetime as well as predict the time intervals for battery replacement. This work provides an ageing study of on commercialized high energy $LiNi_xMn_yCo_{1-x-y}O_2$(NMC)/graphite Li-ion pouch cell cycled under different depth of discharge (DoD). Incremental analysis (IC) was performed on I_t[1]//25 test result to investigate the ageing mechanism and found loss of lithium inventory (LLI) was the main reason causing battery capacity fade. The linear regression observed between the battery state of health (SoH) and partial area loss in IC curves allows the SoH evaluation for cells under different cycling condition within 1% error bound. With the measurement results, the observed phenomena and possible battery degradation mechanism are discussed.

Keywords: Lithium-ion batteries; Incremental analysis; Ageing mechanism, SoH estimation

1 Introduction

In the last decades, Lithium ion (Li-ion) batteries have achieved great success in the portable electronics industry and gained increased interest in the field of electric vehicles (EVs) owing to properties such as high energy and power density, nearly 100% Coulombic efficiency and a lack of memory effect [1]. Li-ion batteries show great potential for the large-scale stationary energy storage system (ESS) application as their cost continues to decrease and their safety and working life-time are improving, some analysts even estimate that electric grid applications could eventually create a larger market than vehicles [2][3].

Nowadays, NMC is becoming one of the most promising cathode materials for Li-ion batteries for automotive applications, as it features the advantages of high specific capacity (150 to 200 mAh/g), enhanced cycling

[1] The notation I_t represents the current rate as documented in the standard IEC 61434 and presented by Equation I_t=C/1h [34]

stability, high safety performance, low toxicity and also cost-effectiveness [4]–[6]. However, the research on this type of batteries is insufficient to fully understand their working and ageing behaviour. The work of Bloom et al. [7] analysed the possible degradation mechanisms of NMC Li-ion cells with differential voltage (DV) analysis and found the lithium loss mainly occurred on the negative electrode, which leads to the capacity degradation. Zeng et al. [8] performed a post-mortem analysis on the NMC/graphite battery after cycling and found that the structure of the positive electrode (PE) was destroyed during cycling, leading to a decrease in diffusion rate of Li ion moving in/out from PE. They also observed a significant increase in both ohmic and polarization resistances because of the electrolyte consumption and possible blockage of separator pores. It should be noted that, these research objects are manually assembled cells. Niehoff et al. [9] found noticeable differences of the ageing results between self-assembled and commercially available NMC cells, and it leads them to believe that the battery ageing mechanism can be altered due to different manufacturing process. Therefore, it is necessary and important to conduct research on a commercial cell scale to understand the ageing phenomena of large-scale NMC cells. Li et al. [10] studied the ageing mechanism of 18650 NMC/graphite cells with a nominal capacity of 2.6 Ah and found that the loss of lithium ions and cathode degradation are the main reasons for capacity degradation. Ecker et al. [11] studied the impact of temperature and state of charge (SoC) on the ageing process of a high power NMC/graphite cell (with 6 Ah nominal capacity) and the test results were used to construct a life-time prediction model. Käbitz et al. [12] studied the ageing of NMC/graphite Li-ion pouch cells with a nominal capacity of 10 Ah by considering the impact of temperature and cell voltage. Jalkanen et al. [13] studied the cycle ageing of commercial NMC/graphite pouch cells with 40 Ah nominal capacity. They found Solid-Electrolyte Interface (SEI) layer growth and lithium plating to be the main contributors to the battery capacity loss during cycling, while no signs of structural/chemical changes in the active material from both electrodes were found in the aged cells. Nevertheless, the impact of cycling depth on the NMC/graphite battery ageing was not studied in the previous work in depth.

Incremental capacity (IC) analysis is a conventional approaches for battery ageing mechanism identification as well as battery state of health (SoH) estimation. Incremental capacity is calculated by differentiating the change in battery capacity to the change in terminal voltage during either charging or discharging, as defined in the Eq. (1).

$$\frac{dQ}{dV} = \frac{\Delta Q}{\Delta V} = \frac{Q_t - Q_{t-1}}{V_t - V_{t-1}} \tag{1}$$

where Q_t is the battery capacity at time t. Although both of them can provide similar information, there is a big difference between these methods. With this method, the voltage plateaus on the charging/discharging curve can be transformed into clearly identifiable peaks on the IC curve. The peaks in IC curve represent phase equilibria [14]. Each peak in the curve has its unique features, like intensity and position, and it represents a specific electrochemical process taking place in the cell [15]. The extracted peak values and the shape and position variation of peaks are closely related to the battery capacity fading. The specific degradation mechanism can be distinguished by analysing the progression of each peak in IC curves throughout ageing, observing how the change of the active materials over time can be helpful in identifying the best operating conditions for cells.

This article provides an ageing research on the high energy NMC/graphite cells, IC curves were employed to process the experimental data from the $I_t/25$ test in order to understand the physical battery degradation process. An effective SoH estimation method was proposed based on the IC analysis.

2 Experimental

The commercialized high energy NMC batteries have been used for this research with a nominal voltage of 3.7V. All cycling tests were done at a current rate of 0.5 I_t. Cells were divided into three groups and cycled under different cycling depth (CD). The selected cycling DoD levels are 100%, 80% and 60%, the DoD always refers to the nominal capacity as indicated by the battery manufacturer in this work. The cells cycled under 100% DoD refer to a complete discharge from 100% SoC to 0% SoC and a complete charge process from 0% to 100% SoC with a middle cycle SoC of 50%. Similarly, the cells cycled under 80% DoD refer to discharge and charge process in the SoC range of 100% to 20% with a middle SoC level of 60%, and cells

cycled under 60% DoD are discharged and charged in the range of 100% to 40% SoC with a middle SoC level of 70%. The cells are named after numbers and the cycle test matrix is given in Table 1. All cycle life tests were conducted at room temperature (around 25 °C).

Table 1. Test matrix for cycling ageing

Specifications	Cell Label					
	Cell 1	Cell 2	Cell 3	Cell 4	Cell 5	Cell 6
Cycle depth	100%	100%	80%	80%	60%	60%
Cycling SoC range	100-0%	100-0%	100-20%	100-20%	100-40%	100-40%
Middle SoC	50%	50%	60%	60%	70%	70%

As the battery capacity degrades and the internal resistance increases with the cumulative cycle number, $I_t/25$ test is performed for every testing stage, including the beginning of life (BoL), during cycling and the end of life (EoL) in order to determine the actual cell status and to obtain the degradation information. The purpose of the capacity test at low current rate of $I_t/25$ is to identify the battery ageing mechanism with incremental capacity analysis. At such low constant current, full charge and discharge tests are able to measure the amount of accessible capacity of the cell and to determine the relationship between the cell potential and capacity under quasi-equilibrium conditions. The resulting charge and discharge curves contain electrode phase information with a minimum amount of kinetic artifacts and are well suited for further analysis [1], [14]. The test at BoL allows us to collect the information of the initial condition of the battery, and it determines the baseline values of battery health, which are later used to enable health monitoring throughout the useful life of the battery. The periodic characterization tests performed during cycling intervals allow us to acquire information on the battery ageing trends. The EoL of a battery is established when the remaining rated capacity of the studied system reaches less than 80% of the initial capacity [16]. EoL performance tests can be used to assess potential secondary uses for the battery and destructive test (Post-mortem) can be included since the battery has already reached the EoL [17]. In this test, RPTs have been performed with intervals of every 100 equivalent full cycles.

3 Results and discussion

3.1 Performance degradation of cells

Fig. 1 shows the discharge performance of cell 1 at 0.5 I_t discharge current rate after a certain cycle number. The shape of the discharge curves does not change significantly as the cells age. As shown in the figure, the discharge voltage slightly shifts toward to the lower capacity level during cycling due to battery capacity loss. Two clear voltage plateaus can be identified from the capacity-voltage curves due to phase changes during discharging, which are pointed out by the blue circles. The information about the battery ageing mechanism is hidden behind the shift of voltage plateaus. By applying IC analysis, these voltage plateaus can be transformed into peaks, thus the ageing process and be identified by analysing the change of peaks in IC curves.

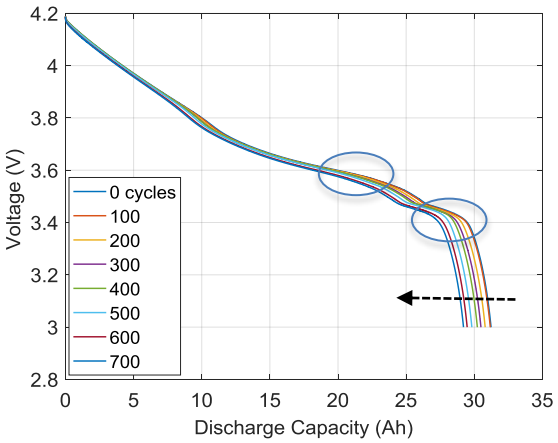

Fig. 1. Discharge voltage evolution curves as function of discharge capacity of cell 1 at different ageing stages

The initial capacity of cells 1 to 6 are 31.23, 31.11, 31.38, 31.39, 31.11 and 31.4 Ah respectively, and the variation of initial capacity among each other is less than 1%. The evolution of the discharge capacity of the six cells as functions of full equivalent cycles at different cycling conditions is presented in Fig. 2 (a). The almost identical change trend of the cell capacity between cells cycled under the same cycling conditions proved the reproducibility of the results. In the following part of this paper, the result of cells 1, 3 and 5 will be chosen for comparison and discussion, as they could be good representations for cells under different cycling conditions. The result of capacity loss of cells 1, 3 and 5 is presented in Fig. 2 (b). The results were normalized to initial capacity values. The capacity loss is represented by Q_{loss}, which can be calculated from Eq. (2):

$$Q_{loss} = \frac{Q_{ini} - Q_t}{Q_{ini}} \tag{2}$$

where $Q_{ini}$is the initial capacity of cells and Q_t represents the actual cell capacity after a period, t. The change trends of the capacity loss from cells cycled under different DoD is out of our expectation, as one would presume the cell with the highest cycling depth would end up as the fasted degradation in the experiment. But the fact that the lower cycling suffers more capacity loss seems counter-intuitive, the possible explanation for this phenomenon will be discussed in the following section.

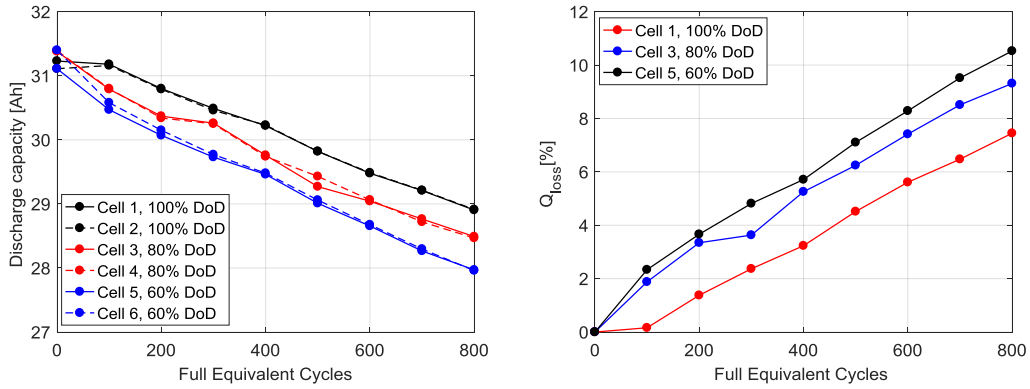

Fig. 2. (a) Evolution of discharge capacity of six tested cells; (b) Comparison of actual capacity loss of Cell 1, 3 and 5 upon cycling as a function of full equivalent cycles

3.2 Cycling ageing analysis by incremental capacity analysis (IC)

Having a good understanding of the battery ageing mechanisms is of significance to maintain battery working performance, safety and long lifetime during operation. Ageing is a phenomenon which leads to loss of capacity or increase in internal resistance in Li-ion batteries during both cycling and storage. Ageing occurs due to various side reactions inside the cell [18]. According to the previous research, the ageing mechanisms for Li-ion cells can be categorized into the following groups: (1) loss of lithium inventory (LLI), (2) loss of active material (LAM) and (3) resistance increase (RI) [19]. It has been well established that dominant ageing mechanisms on graphite anodes are caused by SEI formation, which leads to a significant increase of the impedance, a limitation of the electrode kinetics and LLI. LAM can originate from three basic set of conditions: structural changes during cycling, chemical decomposition or dissolution reactions of transition metal into the electrolyte solution and surface film modification [13] [19]. RI can occur due to the growth of passive films on the surface of active electrode materials [19].

3.2.1 Degradation mechanism identification

Herein, we use the IC analyses with a very low current rate (I_t/25) to acquire more information of the aging mechanism associated with the cycling of this cell. IC analysis investigates the derivative of normalized capacity with respect to the voltage. With this method, the voltage plateaus on the charging/discharging curve with a slow current rate (I_t/25 test) can be transformed into clearly identifiable peaks on the IC curve. The specific degradation mechanism can be distinguished by analysing the progression of each peak in IC curves throughout ageing, seeing how active materials change over time will be helpful for exploiting the best

operating conditions for cells. Each peak in the IC curve has its unique features, such as shape, intensity and position. Each peak presents a specific electrochemical process taking place in the cell [15]. The extracted peak values and the shape and position variation of peaks are closely related to the battery capacity fading.

Fig. 3 shows the discharge curve and an IC curve of fresh cell at room temperature. Five main peaks can be observed from the IC curves. The five peaks have their initial maximum of intensity at 3.85 V, 3.63 V, 3.60V, 3.57 V and 3.47 V, which were marked with peak 1, 2, 3, 4 and 5, respectively. The five peaks will be further used as features of interest (FOI) for analysis, the change of their intensity and positions will be recorded in order to collect the information about cell degradation mechanisms.

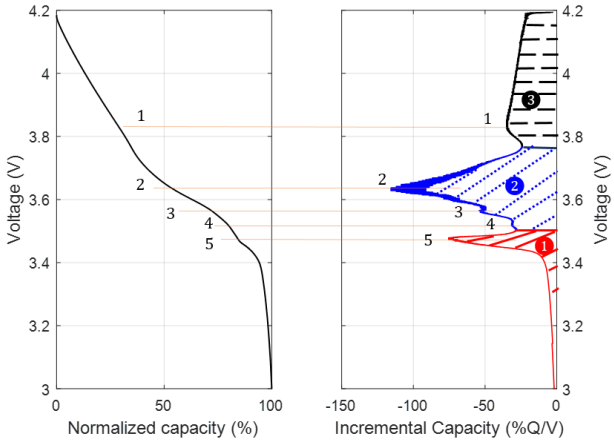

Fig. 3. Cell voltage constant current charge voltage curves and the IC curves of the fresh cell

The IC curves for cell 1, 3 and 5 at different ageing states are illustrated in Fig. 4 (a), (b) and (c), respectively. The most distinctive feature is the evolution of peak intensity and position associated with peaks at the high SoC (peak 1 and 2) as the intensity of the two peaks decreased along with cycle numbers. In addition, peak 3 was formed after 100 cycles and the intensity is decreasing along cycles until it disappeared after 600 cycles. No obvious change of peak intensity was observed for peak 4 and 5, showing that there is no obvious loss of active material from a negative electrode (NE), otherwise which is supposed to be reflected by a change of all the peaks in IC curves [1]. Despite the evolution in peak intensity, the positions of all peaks were shifted toward a higher voltage level. It should be noted that peak 5 is a useful indicator for the Li content in graphite and Li intercalation kinetics [20]–[22]. Peak 2 may represent the sequential phase transition process $Ni^{2+} \rightarrow Ni^{3+} \rightarrow Ni^{4+}$ in NMC cathode [20] [22]–[25]. The area under each peak represents the capacity of the related reaction during the cycling process [1]. The FOIs will be further used as features of interest for analysis, the change of their intensity and positions will be recorded to collect the information about cell degradation mechanisms.

The intensity decrease of the peaks at high potential level suggest a change in the internal balancing the cell, consistent with lithium loss inventory (LLI) due to side reactions with NE [26][27]. The shift of peaks toward higher voltage level, which is also consistent with LLI, suggests decreased potential of negative electrode during cycling. It was also reported by Ref. [1][15] that the simultaneous shift of all peaks and valleys toward higher potentials with ageing indicates an increase of SEI resistance. The shoulder of the IC curve at around 4.18 V is lightly moving up, the decreased intensity indicates that the positive electrode (PE) is becoming less recharged during cycling [23]. Loss of active material (LAM) on the PE side could not be identified from the aforementioned IC analysis on a full cell, which requires further post-mortem analysis.

Cells 1, 3 and 5, have been subjected to life cycle test under different cycling depth, display similar IC features. The comparison of the IC curves from the three cells after 800 full equivalent cycles were illustrated in Fig. 4 (d). Several differences can clearly be observed. For cells cycled under higher DOD range (Cell 5), the intensity of all the peaks is lower than the cells cycled under lower DOD range (Cell 1 and 3). The variation of peak positions was also observed in the three cells, as peak 1 and 2 are located at higher voltage levels for Cell 5 compared to the other two cells. The variation of the peak intensity and position demonstrate the different impact of cycling depth on the ageing process.

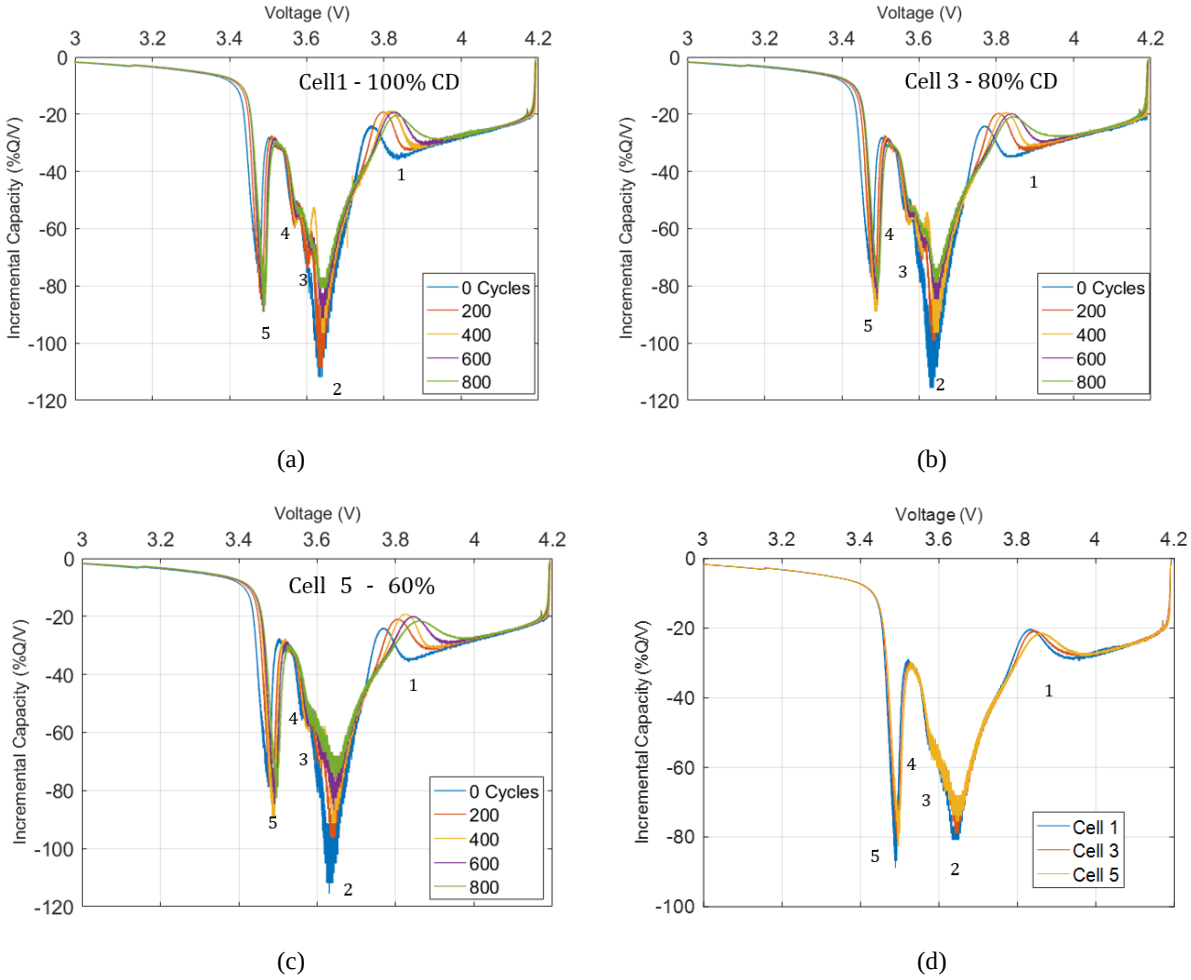

Fig. 4. Representative Incremental Capacity (IC) curves of (a) cell 1 (b) cell 3 (c) cell 5 in the discharge regime at different ageing states, obtained from $I_t/25$ discharge voltage profiles; (d) Comparison of IC curves of cell 1, 3, and 5 after 800 cycles

Later on, the IC peak area is calculated to quantify the ageing mechanism in the test cells. For easy comparison, we separated the area underneath the IC curve into three regions (❶, ❷ and ❸) and marked with different color as shown in Fig. 3. Peak 2, 3 and 4 formed region ❷, and their area are calculated as an integral part instead of calculating each peak, separately. The calculation process is simplified and the final result is evident enough to support further degradation analysis. The peak area after n cycles, A_n, are calculated by integrating dQ/dV. Therefore, A_n represents the capacity involved in the related reaction in this region. The peak area loss can be determined based on Eq. (3):

$$A_{loss} = \left(\frac{A_0 - A_n}{A_0}\right) \cdot 100\% \tag{3}$$

where A_0 means the peak area at BoL. Fig. 5 (a) (b) and (c) compare the evolution of area loss from region ❶, ❷ and ❸ as a function of cycle number for cell 1, 3 and 5. The areas of region ❶, ❷ and ❸ for a fresh cell were measured to be 5.22± 0.01 Ah, 15.22± 0.01 Ah and 11.87± 0.01 Ah, respectively, from the initial reference C/25 tests. The initial capacity of the fresh cell measured at $I_t/25$ was 32.3 Ah, and region ❶ approximately corresponds to 16.1%, region ❷corresponds to 47.1% while region ❸ corresponds to 36.7% of the full capacity.

For all three cells, the area of region ❶ and ❷ show little change, this again confirms that there is almost no loss of graphite negative electrode material. A close look at the area changes between region ❶ and ❷ suggests that the decrease area of region ❷ is made up with the gain of region ❶. The overall area of region

❶ and ❷ remains rather constant as shown in Fig. 5 (d), which suggests that the total capacity delivered by region ❶ and ❷ stays almost unchanged compared with the fresh cell. The shift of the area between region ❶ and ❷ implies that the extent of Li depletion in the NE have been redistributed from reaction ❶ to ❷ over cycle aging[23]. Therefore, the amount of Li involved in the region ❶ is reducing through cycling[23].

The area of region ❸ of all three cells show a big drop after 800 cycles as shown in Fig. 5 (c). The change of this region is mainly caused by LLI according to the previous discussion. Cell 5 cycled under the lowest cycling depth of discharge (DoD) shows fastest area loss in this region, which suggests more cyclable lithium is consumed by the side reactions in Cell 5 compared to Cell 1. It should be noted that the factors of calendaring ageing effect and cycling middle SoC are not considered in this test. Cells cycled at lower cycling depth normally need more time to finish the programmed 100 full equivalent cycles, it's well known that the main degradation mechanism of calendaring ageing is LLI. We could suspect that the calendaring ageing has more negative impact on the capacity fade than the cycling ageing. Similar results can be found in the ageing study of Ecker et al. [11] on NMC/graphite cell, it shows that the battery capacity fades faster during storage compared with the battery cycled at a worse condition, which means cycling can enhance the battery resistive life. Additionally, Cell 5 was experiencing the highest cycling middle SoC and the research in [11] shows that NMC/graphite batteries cycled under higher middle SoC show much faster capacity degradation rate than the cells cycled under lower middle SoC. It's therefore reasonable to suspect that the fastest capacity degradation of Cell 5 might be caused by the calendaring ageing and high cycling middle SoC. However, the influence of middle SoC on battery cycle life-time is not in the scope of this research. The unexpected phenomenon of cells cycled under lower cycling DoD is experiencing faster ageing rate could be explained by higher cycle middle SoC and longer calendaring time, but further research on calendaring ageing and impact of different cycle middle SoC on ageing process need to be carried out to prove this point.

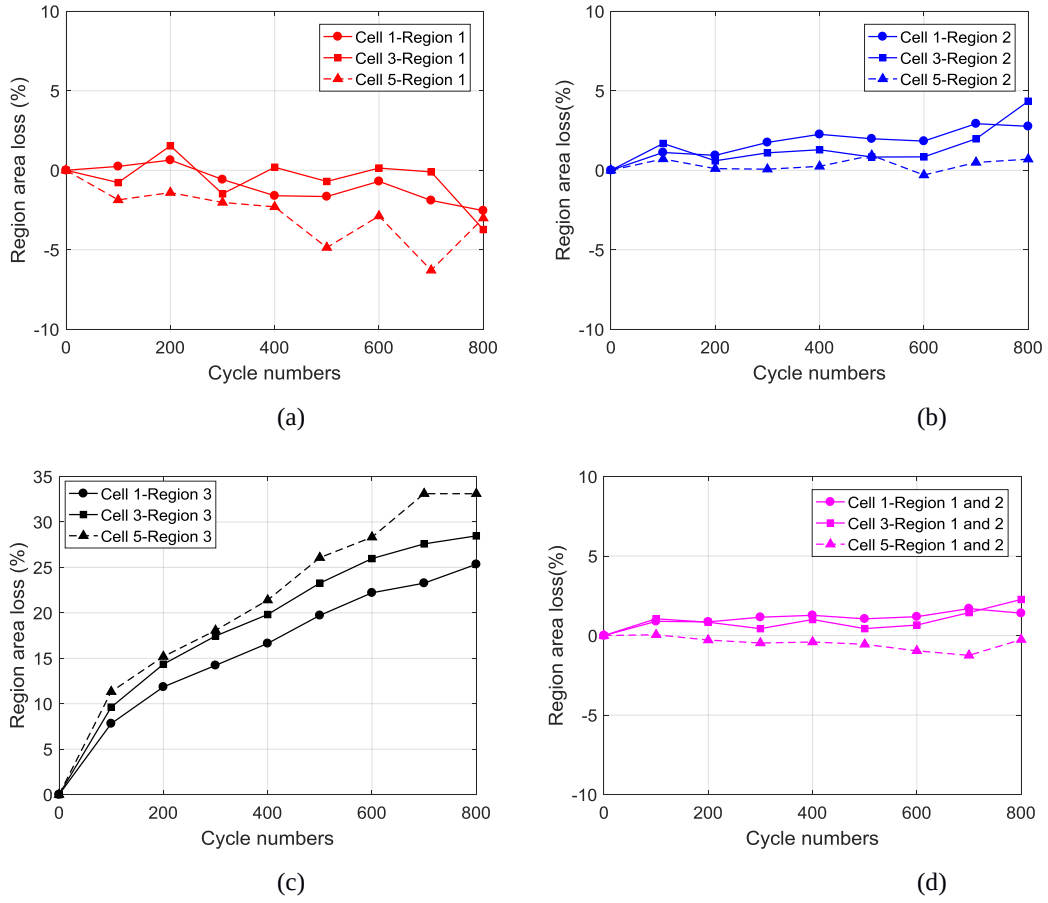

Fig. 5. Region area loss from for (a) region ❶ (b) region ❷ and (c) region ❸ (d) sum of region ❶ and ❷ from cell 1,3 and 5 as a function of cycle number.

The above IC analysis together with the peak area tracing revealed that the cycle ageing of the NMC/graphite cells is mainly the result of LLI caused by consumption of cycleable lithium [28]. We suspect that the reduced amount of Li-ions were consumed by parasitic reaction, mostly like formation and growth of SEI layer on the surface of NE [28]. This result is in agreement with the previous research in Ref. [28][23][29]. LAM on NE is not observed from IC analysis, while LAM on PE cannot be observed from the aforementioned test. The previous research about LAM of NMC containing cells are quite controversial. Some groups suggest LAM on the positive electrode to be a plausible degradation mechanism of for NMC cells due to the dissolution reaction of manganese in positive electrode with hydrogen fluoride (HF) and the formation of $LiMn_2O_4$ [23], [28], [30]–[32], and the manganese dissolution was further confirmed by post-mortem analysis on 18650 NMC/graphite cells in the study presented by Waldmann et al. [33]. The dissolved transition metals are transported through the electrolyte and deposited on the surface of graphite, their incorporation into the SEI layer leading to increased SEI growth and the loss of Li-ions [28]. On the other hand, Jalkanen et al. [13] did not find any signs of structural/chemical changes of the active material from both negative and positive electrodes from post-mortem analysis on aged NMC/graphite cells.

The above IC analysis together with the peak area tracing revealed that the cycle ageing of the NMC/graphite cells is mainly the result of LLI caused by consumption of cycleable lithium [28]. We suspect that the reduced amount of Li-ions were consumed by parasitic reaction, mostly like formation and growth of SEI layer on the surface of NE [28]. This result is in agreement with the previous research in Ref. [28][23][29]. LAM on NE is not observed from IC analysis, while LAM on PE cannot be observed from the aforementioned test. The previous research about LAM of NMC containing cells are quite controversial. Some groups suggest LAM on the positive electrode to be a plausible degradation mechanism of for NMC cells due to the dissolution reaction of manganese in positive electrode with hydrogen fluoride (HF) and the formation of $LiMn_2O_4$ [23], [28], [30]–[32], and the manganese dissolution was further confirmed by post-mortem analysis on 18650 NMC/graphite cells in the study presented by Waldmann et al. [33]. The dissolved transition metals are transported through the electrolyte and deposited on the surface of graphite, their incorporation into the SEI layer leading to increased SEI growth and the loss of Li-ions [28]. On the other hand, Jalkanen et al. [13] did not find any signs of structural/chemical changes of the active material from both negative and positive electrodes from post-mortem analysis on aged NMC/graphite cells.

3.2.2 SoH estimation

An obvious reduction of the area from region ❸ were observed in IC curves as illustrated in Fig. 5. Hence, it was chosen as the feature of interest (FOI) to track their evolution with SoH of battery cell. The SoH values were calculated from capacity test conducted on each cell at the end of each test cycle and the SoH is defined as the ratio of actual cell capacity at a time t (Q_t)to the cell initial capacity (Q_0), as shown in Eq. (4).

$$SoH = \frac{Q_t}{Q_0} = 100\% - Q_{loss}(\%) \tag{4}$$

For a fresh cell, the SoH is equal to 100% and the value of SoH decreases with ageing. Generally, we define the cell end of life (EoL) is when SoH is equal to 80% (capacity loss is 20%). The correlation between the region ❸ area loss and the SoH of each cell from capacity test is illustrated in Fig. 6. The solid line in the figure is the fitted linear relationship between the two values from the tested cells while the dotted line represents the error boundary of $\pm 1\%$. This figure proves the strong linear relationship between the area loss with SoH, and the small deviations between the points with estimated curve within 1% confirms the validity of using region ❸ area loss as the battery SoH indicator. The SoH of the cells cycled under different conditions can all be well estimated from this linear curve, this indicates the generality of this SoH estimation method. In order to get this region area data, only partial discharging test is required with this estimation technique. For a fresh cell, the area of region ❸ can be obtained by discharging from 100% SoC to 60% SoC. Therefore, the test time for IC analysis can be largely decreased with this method. It shows a good potential for the further online SoH estimation. The SoH estimation algorithm proposed in this work can not only provide an accurate SoH estimation within 1% error, but also provides a good link between SoH estiamtion with the real battery degradation mechanism.

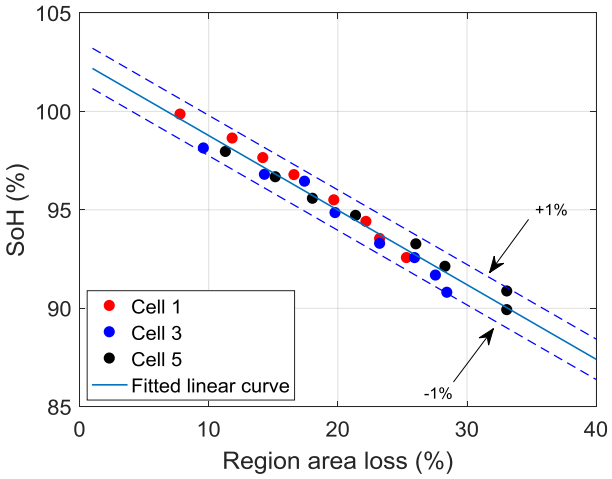

Fig. 6. Correlation between the area loss of Region ❸ and the SoH of the batteries cycled under different DoD

4 Conclusion

In this study, commercial high energy NMC/graphite pouch cells were cycled under different cycling depths at room temperature. This study provides general information about the working and ageing behaviours of this battery type and provides an understanding of their degradation process.

It was observed that the cells cycled under lower DoD range, but with a higher middle SoC were experiencing faster capacity fade. By using non-destructive methods, mainly based on IC analysis and evolution of the IC peak area, we were able to decipher the main contribution to the capacity fading of this commercial NMC cell, which is caused by LLI, while there was no clear loss of active material on the negative electrode. From the obtained result, we could speculate that lower cycle depth can lead to a higher content of LLI due to longer calendar ageing time and higher middle SoC level under this cycling mode. Although the definitive degradation process in the cells still needs to be confirmed by a further post-mortem analysis. The results from IC analysis shows a linear regression between the area loss of region ❸ and the battery SoH, this allows us to evaluate the SoH of batteries cycled under different conditions with less than 1% error. This method can be performed with only partial discharge process and therefore the test time is largely reduced, it shows great potential for real applications.

This work is based on a one and half years continuous cycling test and fully characterization tests on high energy NMC cells. The cells will keep cycling until reaching the EoL, which are expected to be cycled for another one and half years. Till then, post-mortem analysis will be performed on the dead cells in order to have a better understanding of the ageing of this type of batteries. In the future work, IC analysis will be performed on the batteries with different current rate to find the optimal test values which can allow the best and quickest SoH estimation result with a good compromise between time and accuracy. More ageing stress factors will be considered on the life-time of lithium ion batteries like calendaring ageing, cycling middle SoC, temperature and cycling current rate, etc. A holistic ageing model will be developed by considering all the ageing stress factors, which will be helpful for estimating the available life-time of batteries under different conditions and also for operating the batteries under the most desirable modes to reach the longest life-time.

References

[1] X. Han, M. Ouyang, L. Lu, J. Li, Y. Zheng, and Z. Li, “A comparative study of commercial lithium ion battery cycle life in electrical vehicle: Aging mechanism identification,” *J. Power Sources*, vol. 251, pp. 38–54, 2014.

[2] T. Xu, W. Wang, M. L. Gordin, D. Wang, and D. Choi, “Lithium-ion batteries for stationary energy storage,” *Jom*, vol. 62, no. 9. pp. 24–30, 2010.

[3] B. Diouf and R. Pode, “Potential of lithium-ion batteries in renewable energy,” *Renew. Energy*, vol. 76, pp. 375–380, Apr. 2015.

[4] S.-L. Wu *et al.*, “High Rate Capability of Li(Ni1⁄3Mn1⁄3Co1⁄3)O2 Electrode for Li-Ion Batteries,” *J. Electrochem. Soc.*, vol. 159, no. 4, p. A438, 2012.

[5] X. Li *et al.*, “Atomic layer deposition of solid-state electrolyte coated cathode materials with superior high-voltage cycling behavior for lithium ion battery application,” *Energy Environ. Sci.*, vol. 7, p. 768, 2014.

[6] H. Yoshizawa and T. Ohzuku, “An application of lithium cobalt nickel manganese oxide to high-power and high-energy density lithium-ion batteries,” *J. Power Sources*, vol. 174, no. 2, pp. 813–817, 2007.

[7] I. Bloom, L. K. Walker, J. K. Basco, D. P. Abraham, J. P. Christophersen, and C. D. Ho, “Differential voltage analyses of high-power lithium-ion cells. 4. Cells containing NMC,” *J. Power Sources*, vol. 195, pp. 877–882, 2010.

[8] Y. W. Zeng, “Investigation of LiNi1/3Co1/3Mn1/3O2 cathode particles after 300 discharge/charge cycling in a lithium-ion battery by analytical TEM,” *J. Power Sources*, vol. 183, no. 1, pp. 316–324, 2008.

[9] P. Niehoff, E. Kraemer, and M. Winter, “Parametrisation of the influence of different cycling conditions on the capacity fade and the internal resistance increase for lithium nickel manganese cobalt oxide/graphite cells,” *J. Electroanal. Chem.*, vol. 707, pp. 110–116, 2013.

[10] X. Li, J. Kang, and Y. Yang, “A study on capacity and power fading characteristics of Li(Ni1/3Co1/3Mn1/3)O2 based lithium ion batteries,” *Ionics (Kiel).*, pp. 2027–2036, 2016.

[11] M. Ecker *et al.*, “Development of a lifetime predcition moddel for lithium ion batteries based on extended accelerated aging test data,” *J. Power Sources*, vol. 215, pp. 248–257, 2012.

[12] S. Käbitz *et al.*, “Cycle and calendar life study of a graphite|LiNi1/3Mn 1/3Co1/3O2 Li-ion high energy system. Part A: Full cell characterization,” *J. Power Sources*, vol. 239, pp. 572–583, 2013.

[13] K. Jalkanen, J. Karppinen, L. Skogström, T. Laurila, M. Nisula, and K. Vuorilehto, “Cycle aging of commercial NMC/graphite pouch cells at different temperatures,” *Appl. Energy*, vol. 154, pp. 160–172, 2015.

[14] I. Bloom *et al.*, “Differential voltage analyses of high-power, lithium-ion cells 1.,” *J. Power Sources*, vol. 139, no. 1–2, pp. 295–303, 2005.

[15] M. Dubarry and B. Y. Liaw, “Identify capacity fading mechanism in a commercial LiFePO4 cell,” *J. Power Sources*, vol. 194, no. 1, pp. 541–549, 2009.

[16] M. Dubarry, V. Svoboda, R. Hwu, and B. Y. Liaw, “Capacity and power fading mechanism identification from a commercial cell evaluation,” *J. Power Sources*, vol. 165, no. 2, pp. 566–572, 2007.

[17] J. Fan, W. He, C. Hendricks, and M. Pecht, “A Practical Design of Reliability and Performance Test for Portable Lithium-ion Batteries,” no. August, pp. 142–147, 2015.

[18] J. Vetter *et al.*, “Ageing mechanisms in lithium-ion batteries,” *J. Power Sources*, vol. 147, no. 1–2, pp. 269–281, 2005.

[19] A. Barré, B. Deguilhem, S. Grolleau, M. Gérard, F. Suard, and D. Riu, “A review on lithium-ion battery ageing mechanisms and estimations for automotive applications,” *J. Power Sources*, vol. 241, pp. 680–689, 2013.

[20] M. Dubarry *et al.*, “Evaluation of commercial lithium-ion cells based on composite positive electrode for plug-in hybrid electric vehicle applications. Part I: Initial characterizations,” *J. Power Sources*, vol. 196, no. 23, pp. 10328–10335, 2011.

[21] M. Dubarry *et al.*, “Evaluation of Commercial Lithium-Ion Cells Based on Composite Positive Electrode for Plug-In Hybrid Electric Vehicle Applications III. Effect of Thermal Excursions without Prolonged Thermal Aging,” *J. Electrochem. Soc.*, vol. 160160, no. 11, pp. 191–199, 2013.

[22] A. D. and B. Y. L. Matthieu Dubarry, “The Value of Battery Diagnostics and Prognostics,” *J. Energy Power Sources*, vol. 1, no. 5, pp. 242–249, 2014.

[23] M. Dubarry *et al.*, “Evaluation of commercial lithium-ion cells based on composite positive electrode for

plug-in hybrid electric vehicle applications. Part II. Degradation mechanism under 2 C cycle aging," *J. Power Sources*, vol. 196, no. 23, pp. 10336–10343, 2011.

[24] W. H. Ryu, S. J. Lim, W. K. Kim, and H. Kwon, "3-D dumbbell-like LiNi1/3Mn1/3Co1/3O 2 cathode materials assembled with nano-building blocks for lithium-ion batteries," *J. Power Sources*, vol. 257, pp. 186–191, 2014.

[25] S. Hu, Y. Li, J. Yin, H. Wang, X. Yuan, and Q. Li, "The effect of different binders on electrochemical properties of LiFePO4/C cathode material in lithium ion batteries," *Chem. Eng. J.*, vol. 237, pp. 497–502, 2014.

[26] M. Kassem, J. Bernard, R. Revel, S. Pélissier, F. Duclaud, and C. Delacourt, "Calendar aging of a graphite/LiFePO4 cell," *J. Power Sources*, vol. 217, p. 574, 2012.

[27] J. V. M. M. Berecibar, F. Devriendt, M. Dubarry, I.Villarreal, N. Omar, W. Verbeke, "Online State of Health estimation on NMC cells based on Predictive Analytics," *J. Power Sources*, vol. 320, pp. 239–250, 2016.

[28] B. Stiaszny, J. C. Ziegler, E. E. Krauß, J. P. Schmidt, and E. Ivers-Tiffée, "Electrochemical characterization and post-mortem analysis of aged LiMn2O4–Li(Ni0.5Mn0.3Co0.2)O2/graphite lithium ion batteries. Part I: Cycle aging," *J. Power Sources*, vol. 251, pp. 439–450, Apr. 2014.

[29] S. F. Schuster *et al.*, "Nonlinear aging characteristics of lithium-ion cells under different operational conditions," *J. Energy Storage*, vol. 1, no. 1, pp. 44–53, 2015.

[30] B. Stiaszny, J. C. Ziegler, E. E. Krauß, M. Zhang, J. P. Schmidt, and E. Ivers-Tiffée, "Electrochemical characterization and post-mortem analysis of aged LiMn 2O4-NMC/graphite lithium ion batteries part II: Calendar aging," *J. Power Sources*, vol. 258, pp. 61–75, 2014.

[31] A. Eddahech, O. Briat, and J.-M. Vinassa, "Performance comparison of four lithium–ion battery technologies under calendar aging," *Energy*, vol. 84, pp. 542–550, 2015.

[32] P. Röder, B. Stiaszny, J. C. Ziegler, N. Baba, P. Lagaly, and H. D. Wiemhöfer, "The impact of calendar aging on the thermal stability of a LiMn 2O4-Li(Ni1/3Mn1/3Co 1/3)O2/graphite lithium-ion cell," *J. Power Sources*, vol. 268, pp. 315–325, 2014.

[33] T. Waldmann, M. Wilka, M. Kasper, M. Fleischhammer, and M. Wohlfahrt-Mehrens, "Temperature dependent ageing mechanisms in Lithium-ion batteries - A Post-Mortem study," *J. Power Sources*, vol. 262, pp. 129–135, 2014.

[34] IEC 61434:1996 , Secondary cells and batteries containing alkaline or other non-acid electrolytes - Guide to designation of current in alkaline secondary cell and battery standards, International Standard, 1996-10-03

Authors

Yi Li obtained her master's degree of Advanced Materials Science from the Bavarian Elite Program in 2015. A joint program by three Bavarian institutions: the Technical University of Munich, the Ludwig Maximilian University of Munich and the University of Augsburg. She is currently a researcher at MOBI (Mobility and AutomotiveTechnology Research) centre, situated at Department of Electrical Engineering at the VUB. Her PhD project is focused on ageing and lifetime estimation of lithium-ion batteries.

Dr. Mohamed Abdel-Monem received the B.Sc. (excellent with honors) and M.Sc. degrees in Electrical Engineering from Helwan University, Cairo, Egypt. Recently, he obtained his PhD degree in August 2016 (with the greatest distinction) at the Department of Electrical Engineering and Energy Technology (ETEC), Vrije Universiteit Brussel (VUB), Belgium. He is a lecturer (on leave) at Helwan University, Faculty of Engineering. Currently, Dr. Mohamed Abdel-Monem is a Senior Researcher at ETEC and MOBI team at VUB. His current research interests include Second-Life Batteries, Electric vehicles, Battery Characterizations, Systems Modelling, Parameter Estimation, Power Electronics, Renewable Energy, Control Systems Energy management strategies and Battery Management System.

Elise Nanini-Maury is expert in electrochemistry at ENGIE Lab Laborelec since 2014. She holds a double engineering degree in material science since 2010 and a PhD degree in electrochemistry since 2014. Before joining ENGIE Lab Laborelec, she worked for industrial companies and academic research centers where she developed new electrodes and electrolytes for different battery systems. She also was responsible of the installation of a battery test laboratory for cells in an academic environment. In her present position, she manages technical projects and is in charge of the technical achievement of projects tasks in various fields of the energy scene, including energy storage in electrochemical systems such as batteries. She is also in charge of technical evaluation of new energy storage products, collaborative projects and is at the interface with research centers and universities for topics related to energy storage.

Prof. Dr. Noshin Omar obtained his M.S. degree in Electronics and Mechanics from Erasmus University College Brussels. He obtained his PhD in 2012 in the department of Electrical Engineering and Energy Technology ETEC, at the Vrije Universiteit Brussel, Belgium.He is the head of the Battery Innovation Center of VUB. Currently he is coordinating several national and European projects in the field of characterisation, electrical, thermal, electrochemical and lifetime modelling of various rechargeable energy storage systems. He was and is still active in various European projects such as SUPERLIB, BATTERIES2020, FIVEVB. He is authors of more than 100 scientific publications.His research interests include characterization, modeling (electrical, thermal, ageing) and system development of electrical double-layer capacitors and batteries in BEV's, PHEV's, HEV's and stationary applications. He is also active in several international

Prof. Dr. Peter Van den Bossche promoted in Engineering Sciences from the Vrije Universiteit Brussel on a thesis "The Electric vehicle, raising the standards". He is currently lecturer at the Vrije Universiteit Brussel. Since more than 15 years he is active in several international standardization committees, currently acting as Secretary of IEC TC69. He has been closely involved in electric vehicle research and demonstration programmes in collaboration with the Vrije Universiteit Brussel and the international associations AVERE and CITELEC, and is now coordinating research projects on battery modeling, always observing the link to standardization development in the field.

Joeri Van Mierlois professor at the Vrije Universiteit Brussels, one of the top universitiesin this field.Prof. Van Mierlo was visiting professor at Chalmers University of Technology, Sweden (2012).He is expert inthe field of Electric and Hybrid vehicles (batteries, power converters, energy management simulations) as well as to the environmental and economical comparison of vehicles with different drive trains and fuels (LCA, TCO).Prof. Van Mierlo was Vice-president of AVERE (2011-2014)(www.avere.org), the European Electric Vehicle Association and board member its Belgian section ASBE (www.asbe.be). He chairs the EPE chapter "Hybrid and electric vehicles" (www.epe-association.org). He is an active member of EARPA(European Automotive Research Partner Association) and member of EGVIA (European Green Vehicle Initiative Association). He is member of the board of Environmental & Energy Technology Innovation Platform (MIP) and chairman of the steering committee of the sustainable mobility platform of ENERGIK.He is IEEE Senior Member and member of IEEE Power Electronics Society (PELS), IEEE Vehicular Technology Society (VTS) en IEEE Transportation Electrification Community.He is the author of more than 500 scientific publications. He is editor in chief of the World Electric Vehicle Journal and co-editor of the Journal of Asian Electric Vehicles and member of the editorial board of "Studies in Science and Technology", "Batteries"? as well as of "ISRN Automotive Engineering".